PERTURBATION OF A TURBULENT FLOW BY A TRIANGULAR HILL

Fernando David Cúñez Benalcázar, fernandodcb@fem.unicamp.br
Erick de Moraes Franklin, franklin@fem.unicamp.br
University of Campinas, Faculty of Mechanical Engineering, Rua Mendeleyev, 200, Campinas, 13083-970, Brazil

Abstract. *Turbulent flows perturbed by low hills are commonly found in industrial and environmental applications. The perturbation introduces new scales in the problem changing the main flow properties. This paper presents an experimental study on a perturbation of fully-developed turbulent boundary layer by a triangular hill. Water flows were imposed over an asymmetric triangular hill fixed on the bottom wall of a rectangular closed conduit, and the flow fields were measured by PIV (Particle Image Velocimetry). From the instantaneous flow fields, the mean velocities and fluctuations were computed, and the shear stress over the ripple and the field of turbulent production were determined. The general behaviors of obtained velocities and stresses are compared to published asymptotic analyses and the shear stress is discussed in terms of bed stability.*

1. INTRODUCTION

Turbulent boundary layers perturbed by hills are frequently found in nature and industry. Some examples are the airflows over hills, ocean waves and desert dunes, and also water flows over aquatic dunes (which have a triangular profile) inside closed conduits. The latter is commonly encountered in industrial applications, such as air-conditioning and petroleum pipelines.The perturbation of the boundary layer introduces new scales in the problem, changing the velocity and the stress distributions along the hill. These changes are of importance for many environmental and industrial applications. For example, to understand the bed instabilities associated with sediment transport.

Over the last decades, many studies have been devoted to the perturbation of a turbulent boundary layer by a low hill (Jackson and Hunt, 1975; Belcher and Hunt,1998; Franklin and Ayek, 2013), improving our knowledge on the subject. Some of them are based on asymptotic methods.

Jackson and Hunt (1975) have presented an analytical analysis on the perturbation of the turbulent boundary layer by a low hill. They divided the perturbed boundary layer in two regions: (i) an inner region, close to the bed, where the time scale for the dissipation of the energy-containing eddies is much smaller than the time scale for their advection, so that this region is in local equilibrium; (ii) an outer region, that is considered far enough from the bed, where the time scale for the dissipation of the energy-containing eddies is much larger than the time scale for their advection; therefore, the flow is not in local-equilibrium. In the inner region, the local-equilibrium condition allows the use models for turbulent stresses. In addition, this region has a small thickness that does not change significantly along the hill, and the perturbations are driven by the pressure field of the outer region. In the outer region, the mean flow is almost unaffected by the shear stress perturbations and a potential solution is expected at the leading order. Jackson and Hunt (1975) found solutions for each region and matched them, obtaining a solution for the perturbation. That composite solution shows that most of the perturbation occurs in the inner region. Hunt et al. (1988) also showed that the maximum of the perturbation velocity occurs in the shear stress layer and that near surface the relative increase of the surface stress is greater than that of velocity.

Recently, Franklin and Ayek (2013) studied the evolution of the shear stress along a triangular profile. Their experimental results showed that the flow is not in local-equilibrium conditions along the upstream face of the ripple.

This paper presents an experimental study on a turbulent channel flow perturbed by a two-dimensional hill of triangular shape. Water flows at two different Reynolds numbers were imposed over an asymmetric triangular ripple with aspect ratio $O(0.1)$ fixed on the bottom wall of a closed conduit, and the flow was measured by PIV (Particle Image Velocimetry). From the flow measurements, mean velocities and fluctuations were computed, so that the shear stress over the ripple and the field of turbulent production were determined. The general behaviors of the flow are compared to published asymptotic analyses and the surface shear stress is discussed in terms of instabilities of a granular bed.

2. EXPERIMENTAL SETUP

The experimental device consisted basically of a water reservoir, two centrifugal pumps, a flow meter, a flow straightener, *5m* long rectangular transparent channel (*160mm* wide by *50mm* high) a settling tank, and a return line, so that the water flowed in a closed loop following the above order of description.

The straightener consisted of a divergent-convergent nozzle filled with glass spheres with a diameter of $d = 3\,mm$, whose function was to homogenize the flow profile. The test section was *1m* long and started at 40 hydraulic diameters (*3m*) downstream of the channel inlet. There was another *1m* long section connecting the test section exit to a settling tank and the return line. Figure 1 presents a schematic drawing of the experimental device.

Two flow rates were employed, *8* and *10m^3/h*, corresponding to cross-section mean velocities $\bar{U}$ of *0.32* and *0.40m/s* and to Reynolds numbers $Re = \bar{U}2H_{eff}/\nu$ of *2.75×10^4* and *3.5×10^4*, where H_{eff} is the distance from the surface of the PVC plates to the top wall of the channel. The regime was hydraulically smooth in all the cases.

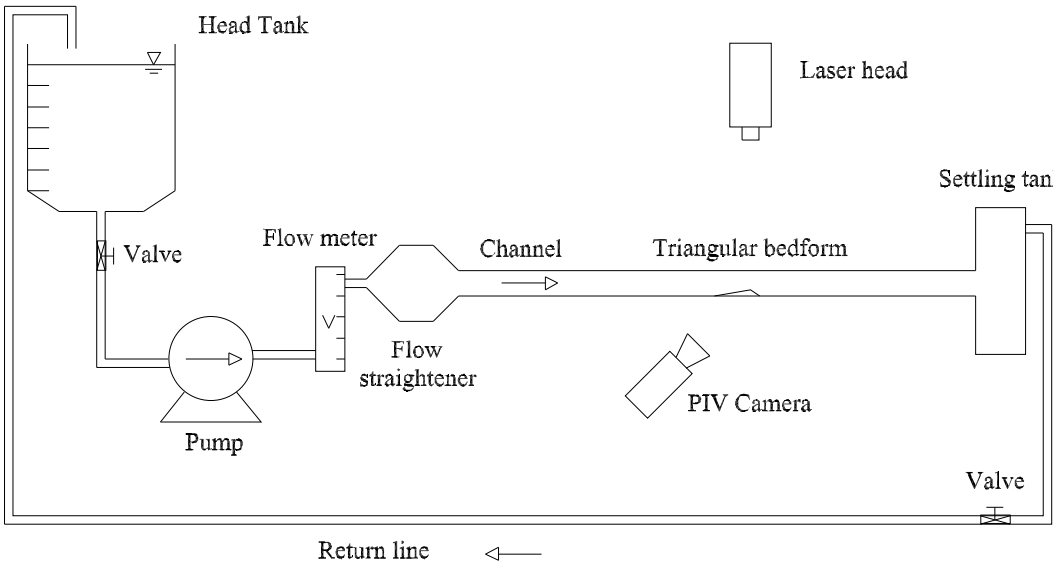

(a)

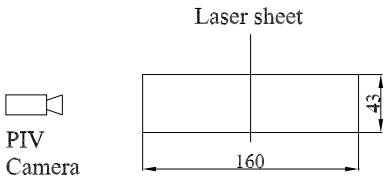

(b)

Figure 1. Layout of the experimental device (a) Side view. (b) Cross section.

PVC plates of *7mm* thickness were inserted in the channel, covering its entire bottom and reducing its height. To model the triangular ripple, a small bed-form of triangular shape was fixed on a PVC plate in the test section (Fig.2). This triangular bed-form had the same scales as the aquatic ripples usually found in environmental and industrial applications.

Measurements were performed without and with the ripple in the closed conduit and were taken at the vertical symmetry plane of the channel. To obtain the instantaneous velocity fields of the flow we used PIV (Particle Image Velocimetry). The employed light source was a dual cavity Nd:YAG Q-Switched laser, capable to emit *2×130mJ* at *15Hz* pulse rate. The power of the laser was fixed at *66%* of the maximum power to assure a good balance between the image contrasts and undesirable reflection from the channel walls. *10μm* hollow glass beads (*S.G. = 1.05*) were employed as seeding particles.

To capture the images we used a *7.4μm × 7.4μm* (*px*^{2}) CCD (charge coupled device) camera with a spatial resolution of *2,048px × 2,048px* and acquiring pairs of images at *4Hz*. The total field employed was of *140mm × 140mm*, corresponding to a magnification of *0.1*, and the employed interrogation area was of *16px × 16px*, corresponding to *1.09mm × 1.09mm*. The computations were made with *50%* of overlap, corresponding to *256* interrogation areas.

The test section was divided in four parts, for each part were acquired *2,000* pairs of images for both flow rates. Fields of instantaneous velocity were computed in fixed Cartesian grids by the PIV controller software (DaVis). MatLab scripts were written to post-process these fields (time-averaged velocity, velocity fluctuations, spatio-temporal averaged profiles, shear velocities, stresses on the ripple coordinate and the turbulent production, for example).

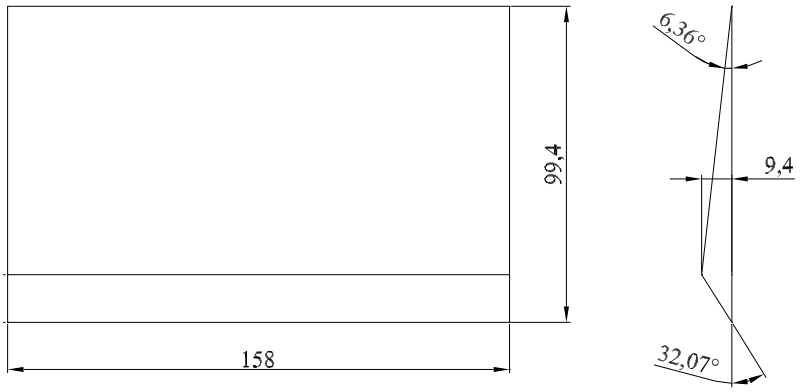

Figure 2. Bedform of triangular profile employed as a model ripple (in the figure, the flow is downward.

3. RESULTS AND DISCUSSION

3.1 Channel flow

Initially, the water flow was measured in the absence of the ripple, corresponding then to a turbulent fully-developed channel flow. For each test, the instantaneous fields were time-averaged and the fluctuation fields (second-order moments) were computed and time-averaged. The time-averaged fields were then space-averaged in the longitudinal direction because the flow was fully developed.The measurements showed that the law of the wall and the Blasius correlation are valid for the turbulent flow in the test section and therefore can be used to estimate the unperturbed flow.

Figure 3 presents the log-normal profiles of the mean velocities for 2 Reynolds numbers. The abscissa is in logarithmic scale and represents the vertical distance from the channel walls walls (bottom or top) normalized by the viscous length, y^+. The ordinate is in linear scale and corresponds to the mean velocities normalized by the shear velocity, ${u_0}^+$.

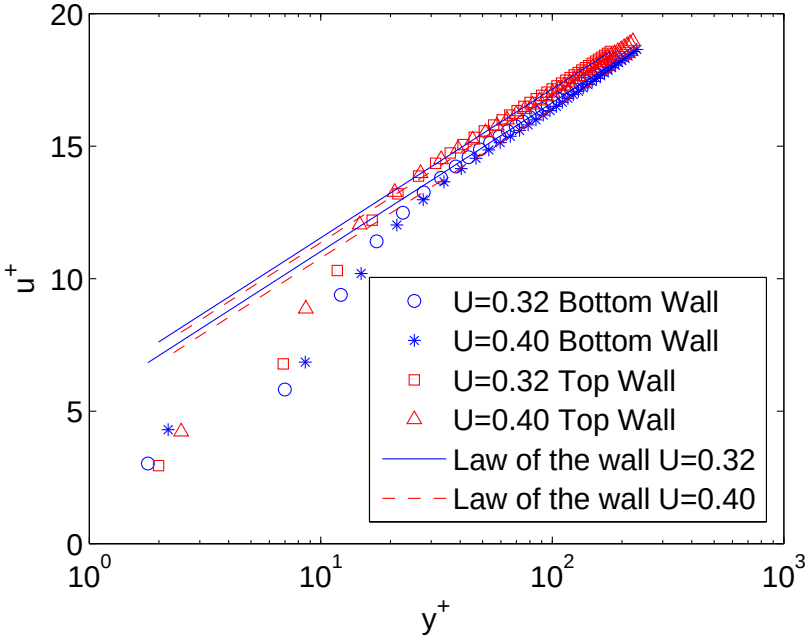

Figure 3. Velocity profiles. The employed $symbols$ are listed in Table 1.

Note that exists a little offset between velocities on the top wall and velocities on the bottom wall. This offset occurs because the experiment's channel is asymmetric. The bottom wall of the channel was covered with PVC plates.

The shear velocity $u_{*,\circ}$ for each Reynolds number was determined by fitting the experimental data in the logarithmic region ($70 < y^+ < 200$). The corresponding values of $u_{*,\circ}$, $B_\circ$ and the friction factor $f_\circ$, as well as the symbols employed in (Fig.3), are presented in Table 1.

In summary, the law of the wall and the Blasius correlation are valid for the unperturbed flow section.

Table 1. Computed shear velocity $u_{*,\circ}$, constant $B_\circ$ and friction factor $f_\circ$ for each water flow rate Q.

$Q(m^3/h)$	$\bar{U}$	Re	*Symbol*	$B_\circ$	$u_{*,\circ}$	$f_\circ$
8	0.32	2.75×10^4	$\circ$	5.41	0.0193	0.0268
8	0.32	2.75×10^4	$\diamond$	5.93	0.0182	0.0237
10	0.40	3.50×10^4	$*$	5.16	0.0237	0.0250
10	0.40	3.50×10^4	$\triangle$	5.75	0.0227	0.0231

3.2 Perturbed flow

The measurements over the model ripple were made for two water flow rates Q=$8m^3/h$ and $10m^3/h$, that correspond to $\bar{U} = 0.32m/s$ and $0.40m/s$ and to $Re = 2.75\times10^4$ and $Re = 3.5\times10^4$. In the following, the perturbed flow is analyzed and compared with the unperturbed flow.

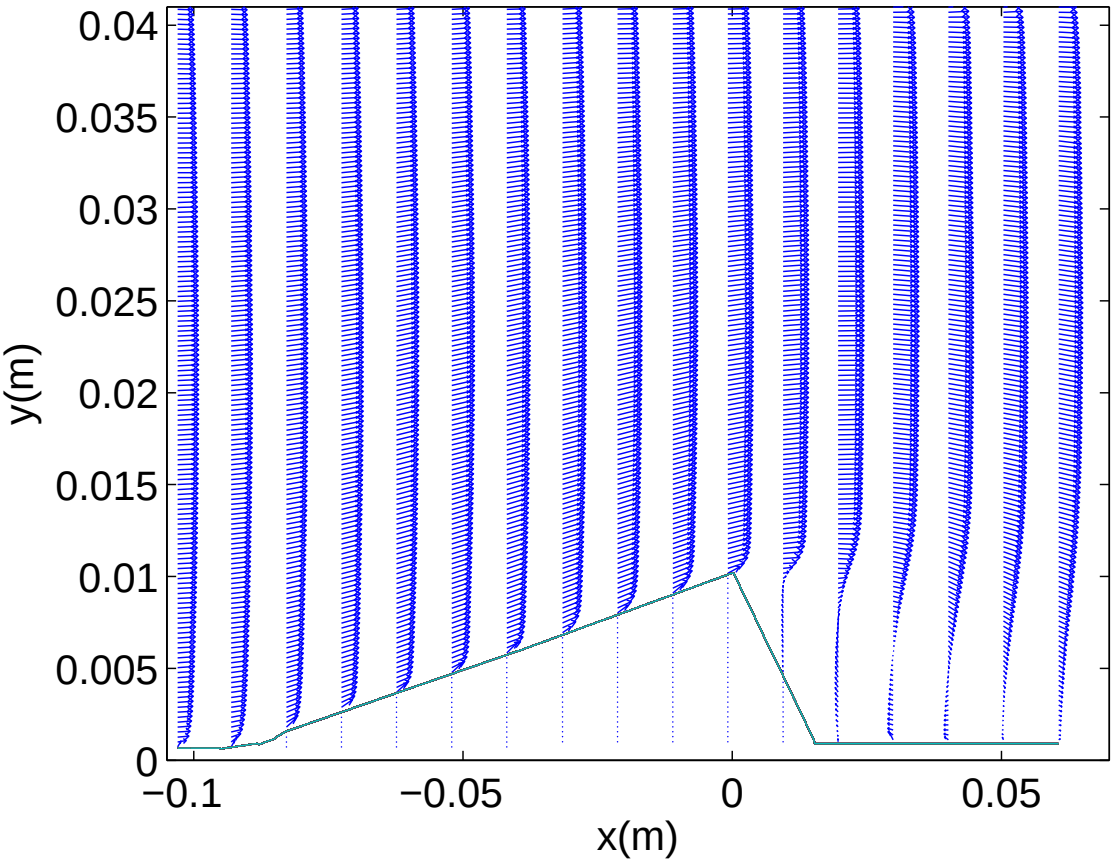

Figure 4. Some profiles of the perturbed mean velocities over the triangular ripple. The flow is from left to right and $Re = 2.75\times10^4$.

Figure 4 shows some mean velocity profiles $\vec{V}(y) = u(y)\vec{i} + v(y)\vec{j}$ over the triangular ripple. A total of 608 profiles were obtained with the spatial resolution of the employed PIV device; however, Fig. 4 presents only 17 of them. Although the smaller number of profiles, this figure allows a better visualization of the flow field. From this figure, we see that the perturbed flow has at least three distinct regions: (i) one far from the ripple surface where the $v \approx 0$ and the perturbation in u is small (given mainly by confinement effects); (ii) other close to the ripple surface and downstream of the crest, where a recirculation bubble exists; (iii) and a third one close to the ripple surface and upstream of the crest, where v is directed upwards and the perturbation of u is stronger than far from the bed.

Figure 5 presents the longitudinal component u of some mean velocity profiles for different longitudinal positions.

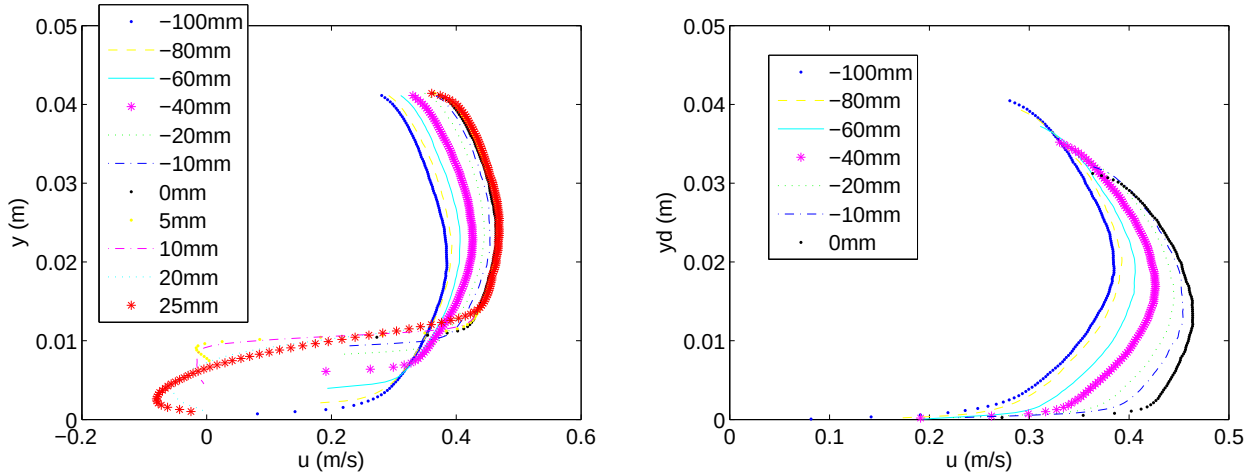

(a) (b)

Figure 5. (a) Longitudinal component of some mean velocity profiles $u(y)$. (b) Longitudinal component of some mean velocity profiles $u(y_d)$. $Re = 2.75\times10^4$.

The employed symbols in the figure are indicated in the legends.

Fig.5a presents y versus u, being suitable for the analysis in the core flow and top wall regions, called upper region.

Fig.5b presents y_d versus u, being suitable for the analysis to the boundary layer in the lower region. This vertical coordinate can be defined as

$$y_d = y - h \tag{1}$$

where $h = h(x)$ is the local height of the triangular ripple and y_d is called displaced vertical coordinate. In $x<0$ region, u increases as the flow approaches the crest and a great part of the perturbation is confined in the lower region.

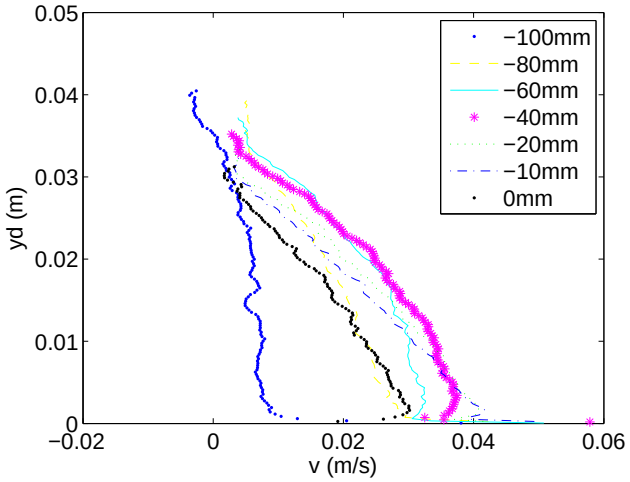

Figure 6. Displaced vertical coordinate y_d versus vertical mean velocity v. $Re = 2.75\times10^4$.

Figure 6 presents the displaced vertical coordinate y_d versus the vertical mean velocity v. The values of v are one order of magnitude smaller than that of u as expected from the dimensional analysis of the perturbation.

Jackson and Hunt (1975) defined the perturbation field as the difference between the flow perturbed and that unperturbed, in the displaced vertical coordinate y_d. This gives:

$$\Delta\vec{V}(y_d) = \vec{V}(y_d) - \vec{V_0}(y_d) \tag{2}$$

where $\vec{V_0}(y_d)$ is the unperturbed flow.

Figure 7a presents some perturbation profiles of the mean velocities along the triangular ripple. Downstream of the crest, the flow detaches and a recirculation bubble is formed. Upstream of the crest, the perturbation is localized in the region $y_d < 2mm$. Fig.7b presents the longitudinal evolution of $|\Delta V|_{max}$ and ${y_d}^+_{|\Delta V|max}$ where ${y_d}^+_{|\Delta V|max}={y_d}_{|\Delta V|max}{}^*u_*/\nu$, then we obtain ${y_d}^+_{|\Delta V|max}<40$. This region corresponds to the buffer and viscous layers of the unperturbed boundary

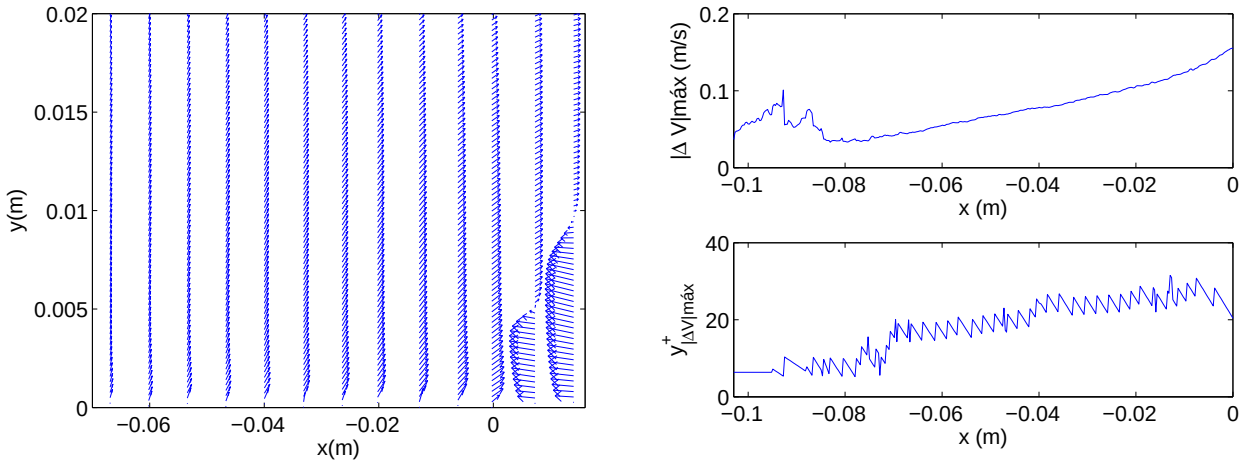

(a) (b)

Figure 7. (a) Some perturbation profiles of the mean velocities *u(y)*. (b) Longitudinal evolution of $|\Delta V|_{max}$ and ${y_d}^+_{|\Delta V|max}$. *Re* = 2.75×10^4.

layer, where the viscous shear stress is very important (Schlichting, 2000). Also we obtain, that the maximum of the perturbation fields $|\Delta V|_{max}$ increases along the ripple, where the maximum occurs on the crest of the triangular ripple.

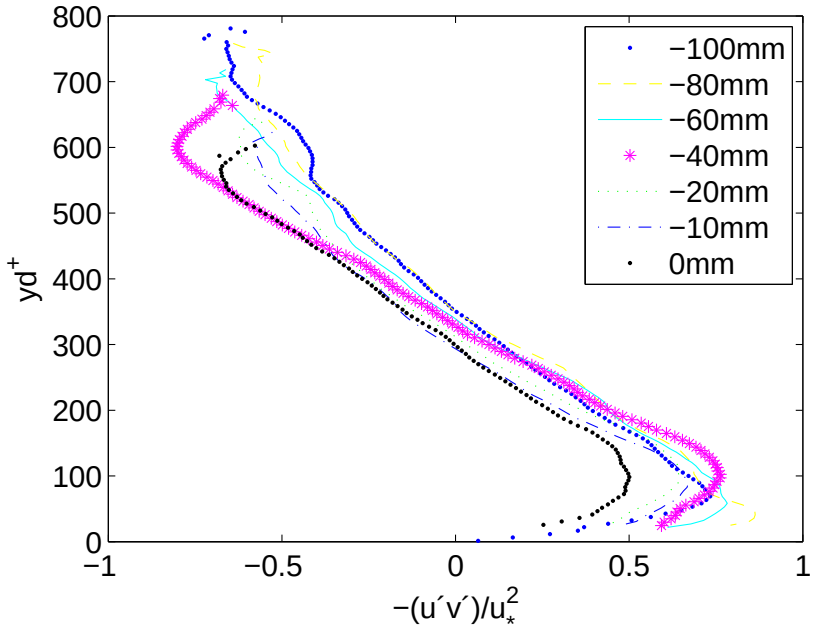

Figure 8. Some profiles of the Reynolds stress *xy* in dimensionless form upstream of the triangular ripple crest: ${y_d}^+$ versus $-\overline{u'v'}/({u_{*,0}}^2)$. *Re* = 2.75×10^4.

Figure 8 presents some profiles of the *xy* component of the Reynolds stresses in dimensionless form, ${y_d}^+$ versus $-\overline{u'v'}/({u_{*,0}}^2)$, upstream of the ripple crest. To decrease the noise, the obtained $-\overline{u'v'}$ profiles were averaged by a sliding window process over closest nine points. Figure 8 shows that the Reynolds stress $-\overline{u'v'}$ is perturbed in the $50 < {y_d}^+ < 250$ region that corresponds to the overlap sublayer of the unperturbed boundary layer. If the flow is in local equilibrium in the ${y_d}^+ < 250$ region, the shear stress on the surface shall scale with $-\overline{u'v'}$ and therefore the longitudinal evolution of $-\overline{u'v'}$ is of importance. Figure 8 also shows that, longitudinally, the perturbation of $-\overline{u'v'}$ decreases near the crest.

Figure 9 presents the longitudinal evolution of the maximum of the *xy* Reynolds stress $(-\overline{u'v'})_{max}$ (for each vertical profile) normalized by ${u_{*,0}}^2$, for the bottom wall region. Figure 9 shows (for each case) that $(-\overline{u'v'})_{max}$ increases approximately *30%* where the triangular ripple starts at $x \approx -0.09m$. For *Re* = 2.75×10^4, $(-\overline{u'v'})_{max}$ decreases in the $0.09m \leq x \leq 0m$ region until $(-\overline{u'v'})_{max} \approx 0.65\ {u_{*,0}}^2$. For *Re* = 3.5×10^4, $(-\overline{u'v'})_{max}$ has a different behavior in the $0.09m \leq x \leq 0m$ region. This cannot be asserted because of the relatively high noise in the data. However we obtain that $(-\overline{u'v'})_{max} \sim$

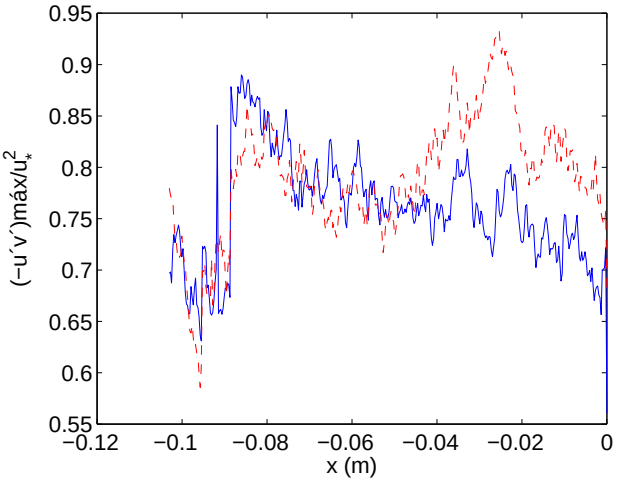

Figure 9. Maximum normalized Reynolds stress $(-\overline{u'v'})_{max}/({u_{*,0}}^2)$ as a function of the longitudinal position x. The *continuous* and *dashed lines* correspond to $Re = 2.75\times10^4$ and $Re = 3.5\times10^4$, respectively.

$O({u_{*,0}}^2)$ in the region analyzed. This indicates that, for the water flow over a triangular ripple (for each case), the region corresponding to the overlap sublayer of the unperturbed flow is in local equilibrium with the lower sublayers.

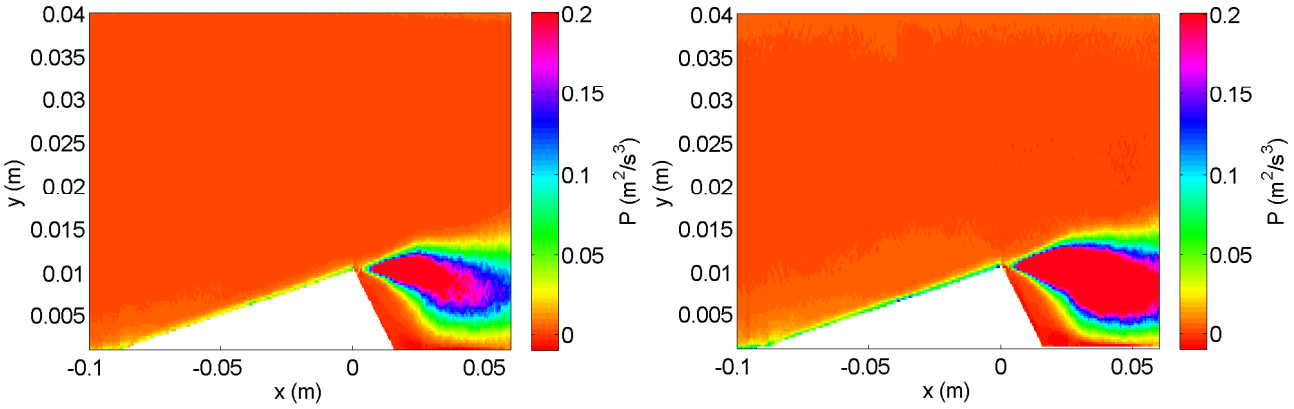

Figure 10. (a) Production of turbulence$Re = 2.75\times10^4$. (b) Production of turbulence $Re = 3.5\times10^4$.

Figure 10 shows the turbulence production upstream and downstream of the ripple crest $Re = 2.75\times10^4$ and $Re = 3.5\times10^4$. The maximum value of turbulence production is obtained where the recirculation region starts. That term is calculated by $P = -\overline{u'v'}(dU_i/dx_i)$. The production term provides the only means by which energy can be passed by the mean flow to the fluctuations. That effect is caused by the vorticity formed in the recirculation region.

4. CONCLUSIONS

This study investigated the perturbation of a turbulent boundary layer by a two-dimensional triangular ripple in the hydraulic smooth regime. The present experiments were performed in moderate Reynolds numbers *(10,000<Re<50,000)*.

The fluid flow was measured by PIV and the obtained mean and turbulent fields were compared with unperturbed flow fields. The *xy* component of the turbulent stress was computed and profiles of $-\overline{u'v'}$ were found.

Along the upstream face of the ripple, the maxima of the turbulent stresses are of the same order of magnitude of the square of the unperturbed shear velocity. In addition, the $-\overline{u'v'}$ vertical profiles decrease slightly until crest of the ripple in the layer corresponding to the overlap layer. Based on these characteristics, it seems that the flow is in local equilibrium in this region.

The main features of the perturbed turbulent boundary layer over a low ripple were confirmed by the experimental results: a recirculation bubble is formed downstream of the ripple crest, shown in Fig.10, and the maximum of the production turbulence was located in the recirculation bubble region. Along the ripple for $Re = 2.75\times10^4$, $(-\overline{u'v'})_{max}$ decreases in the $0.09m \leq x \leq 0m$ region until $(-\overline{u'v'})_{max} \approx 0.65\ {u_{*,0}}^2$, in this region the flow is in local-equilibrium allowing the use models for turbulent stresses, and the maximum of the perturbation velocity occurs in the shear stress

layer where ${y_d}^+_{|\Delta V|max}$<40.

5. ACKNOWLEDGEMENTS

Fernando David Cúñez Benalcázar is grateful to SENESCYT (Programa de Becas Convocatoria Abierta 2014 Segunda Fase), Erick de Moraes Franklin is grateful to FAPESP (grant no. 2012/19562-6) and to CNPq (grant no. 471391/2013-1) for the provided financial support.

6. REFERENCES

Belcher, S.E. and Hunt, J.C.R.,1998, "Turbulent flow over hills and waves", Ann. Rev. Fluid Mech. Vol.30, pp. 507-538.
Franklin, E.M. and Ayek, G.A.,2013, "The perturbation of a turbulent boundary layer by a two-dimensional hill", Journal of the Brazilian Society of Engineering and Mechanical Sciences, Vol.35, pp. 337-346.
Hunt, J.C.R., Leibovich, S. and Richards, K., 1988, "Turbulent shear flows over low Hills",Quart. J. R. Met. Soc. Vol.114, pp. 929-955.
Jackson, P.S. and Hunt, J.C.R., 1975, "Turbulent wind flow over a low hill",Quart. J. R. Met. Soc. Vol.101, pp. 1435-1470.
Schlichting, H., 2000, "Boundary-layer theory", Springer.

7. RESPONSIBILITY NOTICE

The author(s) is (are) the only responsible for the printed material included in this paper.